Published in final edited form as:
J Mol Biol. 2010 April 2; 397(3): 752–766. doi:10.1016/j.jmb.2010.01.064.

Antigenic Characteristics of Rhinovirus Chimeras Designed *in silico* for Enhanced Presentation of HIV-1 gp41 Epitopes

Mauro Lapelosa[1,2,3], **Gail Ferstandig Arnold**[2,3,*], **Emilio Gallicchio**[1,2], **Eddy Arnold**[2,3], and **Ronald M. Levy**[1,2]

[1]BioMaPS Institute for Quantitative Biology, Rutgers University, Piscataway, NJ 08854, USA

[2]Department of Chemistry and Chemical Biology, Rutgers University, Piscataway, NJ 08854, USA

[3]Center for Advanced Biotechnology and Medicine, Rutgers University, Piscataway, NJ 08854, USA

Abstract

The development of an effective AIDS vaccine remains the most promising long-term strategy to combat human immunodeficiency virus (HIV)/AIDS. Here, we report favorable antigenic characteristics of vaccine candidates isolated from a combinatorial library of human rhinoviruses displaying the ELDKWA epitope of the gp41 glycoprotein of HIV-1. The design principles of this library emerged from the application of molecular modeling calculations in conjunction with our knowledge of previously obtained ELDKWA-displaying chimeras, including knowledge of a chimera with one of the best 2F5-binding characteristics obtained to date. The molecular modeling calculations identified the energetic and structural factors affecting the ability of the epitope to assume conformations capable of fitting into the complementarity determining region of the ELDKWA-binding, broadly neutralizing human mAb 2F5. Individual viruses were isolated from the library following competitive immunoselection and were tested using ELISA and fluorescence quenching experiments. Dissociation constants obtained using both techniques revealed that some of the newly isolated chimeras bind 2F5 with greater affinity than previously identified chimeric rhinoviruses. Molecular dynamics simulations of two of these same chimeras confirmed that their HIV inserts were partially preorganized for binding, which is largely responsible for their corresponding gains in binding affinity. The study illustrates the utility of combining structure-based experiments with computational modeling approaches for improving the odds of selecting vaccine component designs with preferred antigenic characteristics. The results obtained also confirm the flexibility of HRV as a presentation vehicle for HIV epitopes and the potential of this platform for the development of vaccine components against AIDS.

Keywords

vaccine design; monoclonal antibody 2F5; chimeric virus; reorganization free energy; protein binding

[*]*Corresponding author*. Department of Chemistry and Chemical Biology, Rutgers University, Piscataway, NJ 08854, USA. gfarnold@cabm.rutgers.edu.

Supplementary Data

Supplementary data associated with this article can be found, in the online version, at doi:10.1016/j.jmb.2010.01.064

Introduction

An effective *acquired* AIDS vaccine would be a crucial component of any long-term strategy to combat human immunodeficiency virus (HIV)/AIDS. However, designing immunogens that can elicit effective, broadly neutralizing responses against HIV has been a surprisingly difficult task. This highlights the need for novel alternative approaches aimed at the discovery of effective AIDS vaccines.[1] Some of the most promising target epitopes of HIV are located in the membrane-proximal external region (MPER) of the transmembrane component of the envelope glycoprotein gp41 of the virus. The MPER plays an important role in the process of HIV fusion to the host cell membrane,2،3 as well as in permitting CD4-independent transcytosis of the virus across epithelial cells at mucosal surfaces.2 These functions likely explain sequence conservation of this region and the efficacy of antibodies directed against it. 3 Potent responses against the MPER are associated with stronger and broader neutralizing capabilities in infected individuals,[4] illustrating the value of including an MPER immunogen in an AIDS vaccine or vaccine cocktail.

A set of epitopes has been identified in the MPER region. These are the ELDKWA epitope (HIV-1 HxB2 gp41 residues 662–667), recognized by the particularly broadly neutralizing human mAb 2F55 and the adjacent residues that bind the broadly neutralizing human mAb 4E106 epitope (HxB2 residues 672–679) as well as the phage display-derived mAb Z13e1 (the IgG version of an affinity-enhanced antigen-binding fragment (Fab) of Z13).7 More recently, two new IgMs, WR316 and WR320, have been identified that bind to this region (HxB2 residues 668–673 and 661–679, respectively) and show some degree of neutralizing activity as well.8

In this study, we focused specifically on the ELDKWA epitope. It has been reported that infected individuals producing neutralizing antibodies directed against the ELDKWA epitope exhibit health benefits.[9,10] While none of the immunogen-induced immune responses generated against this region has been both broadly reactive[11] and potent thus far, we believe that presentations in which the MPER epitopes are preorganized for binding should produce valuable immunogens that can contribute to a successful vaccine.

A promising approach for epitope presentation consists of grafting gp41 MPER epitopes of HIV-1 onto the surface of the safe and highly immunogenic human rhinovirus (HRV),[12] a picornavirus that causes approximately 50% of common colds.4 HRV is likely to be particularly favorable as a vaccine vehicle due to its ability to stimulate potent humoral immune responses, including mucosal immune responses13 as well as T-cell help responses.14،[15] We have shown that HRV can accommodate a variety of foreign sequences[9,10،12] in a surface loop of the viral coat protein 2 of HRV, designated the VP2 puff.11،14 This surface loop is, in fact, part of one of HRV's own immunogenic sites, constituting the largest of three loops forming the neutralizing immunogenic site II (NIm-II15). We demonstrated recently that ELDKWA-derived epitopes can be displayed on HRV in ways that stimulate neutralizing immune responses directed against diverse pseudoisolates of HIV-1.13 These recombinant immunogens have been among the few reported that elicit broad, albeit modest, neutralization of HIV, and we are actively pursuing their further development with the goal of providing protective AIDS vaccine components.

In an earlier study,[16] we used computational modeling techniques to study the effect of presentation modality on the conformational propensity of the ELDKWA epitope on the surface of HRV. We hypothesized that those presentation constructs with the highest fraction of epitope conformations compatible with antibody complexation would present the highest binding affinity for 2F5, making them the most antigenic.

The crystallographic structure of an ELDKWA-based peptide complexed with the Fab fragment of the 2F5 monoclonal antibody (mAb)[17] provided the structural target against which we compared the ensemble of conformations generated by modeling. These studies indicated that the length, the hydrophobic character, and the precise site of insertion of the epitope are crucial for achieving the greatest structural similarity to the target structure.16

In the present study we have used these insights to formulate a new combinatorial library of chimeric rhinoviruses (cHRVs) in an effort to isolate constructs with improved binding affinity with respect to the 2F5 mAb. Immunoselection of the library with a combination of mAb 2F5 and competitive ELDKWA-based peptides resulted in the isolation of specific cHRVs displaying greater affinity for 2F5 than previously designed constructs with respect to both ELISA assays and direct spectroscopic determination of the equilibrium constants for antibody binding. Computer modeling calculations showed that the increased binding affinity of these constructs for 2F5 is correlated directly with their more favorable binding reorganization free energies, a measure of their ability to assume conformations compatible with antibody complexation based on the structural criteria we developed earlier.[16]

The results obtained confirm the flexibility of HRV as a presentation vehicle for HIV epitopes and the potential of this platform for the development of vaccine components against HIV. In the next section we present the results concerning the design, production, and immunoselection of a combinatorial library of cHRVs designed according to the structural insights we presented earlier.[16] This is followed by the results of ELISA assays used to gauge the affinity of specific isolates for 2F5 and the results of more rigorous binding constant determination using spectroscopic measurements for the most promising cHRVs obtained including, for comparison, an ELDKWA-based cHRV characterized previously without the use of computational modeling.[13] The results of computer simulations of the cHRVs are described and discussed, illustrating the importance of the binding reorganization free energy in determining the antigenic characteristics of these constructs.

Results

Design, production, and immunoselection of a new combinatorial library

A focused combinatorial library was generated on the basis of cHRV3, a chimeric HRV predicted by computer modeling to have a favorable affinity for 2F5.[16] The library encoded the ELDKWAS core sequence flanked on either side by amino acids randomized to encode any of the 20 commonly occurring amino acids, enhancing the chances of identifying chimeras with favorable growth characteristics and well presented ELDKWA inserts. The entire cassette (Table 1) was inserted between residues S158 and G163 of the VP2 protein of HRV14. The selection of the genetic modification site was made according to previous studies directed to display foreign sequences on loop 2 of the neutralizing immunogenic site II of HRV14.[9] A library of plasmids was obtained from the pST-LIC vector and a library of oligonucleotides. Subsequently, *in vitro* transcription allowed us to produce infectious RNAs. A pool of chimeric viruses was produced by transfection into H1-HeLa cells, and the transfection efficiency (2.4×10^5 plaque-forming units/μg) was determined by counting the number of plaques obtained after transfection. The chimeric pool was purified so that selected viruses might be more easily purified at later stages. Viral RNAs from three recombinant viruses selected at random were sequenced, confirming the presence of ELDKWAS sequences (data not shown). No HRV residue N-terminal or C-terminal to the ELDKWAS core were either mutated or deleted.

Chimeric viruses obtained from the library were propagated, purified, and immunoselected on the basis of their ability to bind to immobilized mAb 2F5 in the presence of 0–16 pmol of competing peptide (Ac-EQELLELDKWASSLW-NH_2; described in Materials and Methods).

The chimeric viruses thus selected grew at rates comparable to that of wild-type HRV14, indicating that the presence of the inserts was not deleterious to their growth. We observed a non-random preponderance of proline and glycine residues among the flanking residues on both sides of the insert (Table 1). This might be related to structural features of the engineered loop that affect the stability or acceptable folding of the chimeric viruses that are compatible with the ability to bind 2F5.

Assessment of ability of cHRVs to bind mAb 2F5

ELISA experiments—To assess the ability of individual, immunoselected viruses to recognize 2F5, we used indirect competitive ELISAs (detailed in Materials and Methods) and tested the ability of the cHRVs to compete with a 14-mer ELDKWA-containing peptide capable of binding to immobilized 2F5. The B–D and F virus pools were isolated after immunoselection using 16 pmol (B), 8 pmol (C), 4 pmol (D), and 2 pmol (F) of peptide per well. Viruses, B1, C1, D1, F1, and B2 (Table 1) have shown peptide concentration-dependent binding to 2F5, unlike the HRV14 control (Fig. 1), demonstrating that these viruses were able to compete with the 14-mer ELDKWA peptide for binding to 2F5. Indeed, the ELISA results (Fig. 1) indicate that the majority of these viruses have significantly better affinity for 2F5 at all concentrations of peptide tested than the 14-C40-1 chimeric virus, one of the most promising vaccine constructs of this kind characterized to date. B1, selected from the most competitive immunoselection conditions, showed the best binding to 2F5 in the competitive ELISA of all of the individual chimeric viruses tested. Thus, B1 effectively competed with the 14-mer peptide in preferably binding 2F5. C1 and B2 also showed high 2F5 binding affinity compared to the other chimeric viruses tested, which also follows the pattern that the greatest competition with peptide yielded the best binders to 2F5.

The better binding ability of chimeras derived from the combinatorial library relative to 14-C40-1 is consistent with our earlier computational study in which we compared the conformational propensities of the 14-C40-1 insert to that of an insert similar in size and electrostatic character to that of B1.[16] We observed that B1 had greater solvent exposure and fit better in a docking model with the 2F5 Fab (indicating it has a higher propensity to adopt a conformation competent for binding to 2F5 than does the 14-C40-1 chimera). In contrast, the 14-C40-1 chimera was found to be likely to form intramolecular hydrophobic interactions, constraining the exposure of the epitope on the HRV surface.[9]

Fluorescence quenching experiments—We conducted fluorescence quenching experiments (described in Materials and Methods) to obtain a more quantitative measure of the binding affinity than could be obtained from the competitive ELISA experiments. Using this technique, we investigated the B1 and C1 isolates, which were seen to have two of the three most promising ELISA profiles (using the 14-C40-1 virus as a reference). Fluorescence quenching allows accurate thermodynamic analysis of antigen–antibody binding. Quenching efficiency is a measure of the change in the environment in the vicinity of optically active residues (tryptophans) as the complex is formed. The fluorescence quenching titration curve reflects the strength of the interaction of the antigen–antibody complex. Variations in the titration curves can be attributed to differences of affinities of the chimeras for 2F5, which in the cases tested (see below) followed the same trends as in the competitive ELISA (Fig. 1).

Fluorescence quenching measurements were supported by two control assays: increasing concentrations of 2F5 did not alter the background fluorescence of the buffer (data not shown); and the addition of 2F5 did not influence the emission fluorescence of wild-type HRV14. The fluorescence quenching titration data (e.g., see Fig. 2 for B1), were well represented by a non-linear function (described in Materials and Methods) that determines the dissociation constant assuming monovalent binding. Bivalent binding of the antibody at the NIm-II loop has been

excluded on the basis of distances and mutual orientation of the insertion sites on HRV14[13] and the modeled structure of the Fab–virus complex (see below) in which the radial orientation of the Fab with respect to the viral surface directs the other Fab arm of the antibody away from the virus particle and out into solution.

The dissociation constants (K_d) for B1 (2.0±0.68 nM), C1 (23.81±12 nM) and 14-C40-1 (769.23±125 nM) were estimated from the fluorescence data. The relative binding free energies (Table 2) were obtained from the dissociation constants as:

$$\Delta\Delta G_{obs} = RT\ln(K_d^2/K_d^1) \quad (1)$$

where K_d^2 and K_d^1 are the dissociation constants of the given (B1 or C1) and reference virus (14-C40-1), respectively. For comparison, Table 2 gives the approximate binding free energies for the B1 and C1 viruses relative to 14-C40-1 obtained from the competitive ELISA assays. The ELISA binding free energy values are estimated on the basis of the peptide concentration corresponding to A_{450}=0.5 (as described in Materials and Methods). As expected, the ELISA relative binding free energies (Table 2) slightly underestimate the relative binding free energies measured by fluorescence quenching because the immobilization of the antibody in the ELISA assay disables some of the virus–antibody interactions.[18] Nevertheless, the ELISA and fluorescence quenching measurements agree well in terms of the rank order of affinities to 2F5. Among the three chimeras, both measurements indicate that B1 is the strongest binder followed closely by C1, and 14-C40-1 consistently shows a significantly reduced affinity compared to B1 and C1.

Reorganization free energy model of observed binding affinity differences

Conformational reorganization is an important factor in protein recognition and binding. Both binding partners incur a free-energy penalty for reorganizing the ensembles of conformations present in their unbound forms to those compatible with complexation. Binding affinity is enhanced when the binding partners are preorganized to assume binding-competent conformations in their unbound forms. Minimizing the binding reorganization free energy is particularly important in this application because, as opposed to drug design applications where the composition of the inhibitor is optimized relative to the protein target, the epitope sequence is fixed and cannot be varied to enhance the binding affinity.

Earlier, we hypothesized that the binding affinity of the ELDKWA epitope inserted onto HRV for 2F5 is increased when preferentially presenting this epitope in a conformation predisposed for binding.[16] We were able to identify a set of characteristics of chimeric HRV constructs that display the ELDKWA epitope preferentially in the same β-turn conformation as that seen in the crystal structure in complex with 2F5.[19] These characteristics, including the hydrophobic nature and length of the insert as well the central positioning of the DKW epitope core motif within the insert, form the design principles of the combinatorial libraries of chimeric viruses studied in this work.

The aim of the present modeling work was to establish whether the earlier modeling predictions16 are consistent with the measurements of the chimera:2F5 binding affinities described here. In order to generate the corresponding conformational ensembles, the B1 and C1 chimeric viruses were modeled by atomistic parallel molecular dynamics simulations as described (also summarized in Materials and Methods).[16] The ensembles were analyzed in terms of the fraction of conformations compatible with 2F5 binding (described in Materials and Methods). As discussed below, a large population of binding-competent conformations can be related quantitatively to a high level of antibody affinity.

The computational models for the B1 and C1 viruses were generated by homology modeling as described in Materials and Methods. Molecular dynamics simulations were conducted using the parallel REMD conformational sampling method (described in Materials and Methods).[20] The salient simulation results are illustrated in Fig. 3, which shows the C^{α} RMSD values of the ELDKWA motif of the conformers generated at 310 K with respect to the solution NMR structure of a 13-mer peptide containing the ELDKWA motif (1LCX)[21] and the X-ray structure of the MPER-derived 7mer peptide complexed with 2F5 (1TJG).19 The 1LCX peptide NMR structure was reported by Biron *et al*. to be helical in solution,[21] whereas the peptide-Fab crystal structure contains a β-turn conformation.[19] For comparison, Fig. 3 shows the same kind of analysis for the 14-C40-1 chimeric virus which, as described,[16] assumed a more extended, less β-turn-like conformation.

The simulation results (Fig. 3) indicate that the ELDKWA epitope is quite flexible on the surface of the chimeric HRV and that the distribution of conformations is substantially affected by the nature and number of the flanking amino acids (compare Fig. 3a, b, and c, whose sequences are given in Table 1). The majority of conformations from the simulated ensembles of B1 and C1 (Fig. 3a and b) are found in the left region of the plots, indicating that they adopt conformations similar to the target β-turn conformation more often than 14-C40-1 (Fig. 3c), which is rarely found close to the target crystal structure.

These results mirror the binding affinity measurements given in Table 2. In agreement with the reorganization free energy argument discussed above, the chimeras with the greatest population of conformers resembling the target mAb-bound β-turn conformation (B1 and C1) are those with the strongest affinity to 2F5. The ensemble of conformers of C1 is more heterogeneous than that of B1 (demonstrated by the spread of points along the x-axis of Fig. 3a and b). Furthermore, consistent with the weaker affinity of the C1 conformers for 2F5 compared to the B1 conformers, C1 presents a slightly smaller fraction of conformers that are similar to the bound conformation compared to B1.

To quantify these observations, we estimated the 2F5 binding free energy differences for the three constructs, based on the corresponding fractions of conformers in proximity to the target-bound conformation. To this end, we adopted a strict criterion of proximity (described in Materials and Methods) that takes into account, through a backbone angle similarity measure, the correct orientations of the side chains of the DKW epitope core motif that are critical for the formation of the proper antigen–antibody interactions. To estimate the relative binding affinities of the chimeras from the simulation, we express the free energy of binding, ΔG_{bind}, as the sum of the antigen–antibody interaction energy, ΔE_{int}, and the binding reorganization free energy, ΔG_{reorg}:

$$\Delta G_{bind} = \Delta E_{int} + \Delta G_{reorg} \tag{2}$$

where:

$$\Delta G_{reorg} = -kT \ln P \tag{3}$$

and P is the fraction of conformers that are structurally similar to the bound ELDKWA peptide in complex with 2F5. Assuming that ΔE_{int} variations are small in this case, based on the fact that the residues involved in the epitope/2F5 paratope are the same in all three chimeric viruses, the relative binding free energies are mostly reduced to the difference of reorganization free energies. It follows that the relative binding free energy between viruses 1 and 2 is given by

$$\Delta\Delta G_{bind} \approx -kT\ln P_2/P_1 \quad (4)$$

where P_1 and P_2 are the populations of the binding-competent macrostates of viruses 1 and 2, respectively. The population of the binding-competent macrostates is computed using a definition involving both RMSD and backbone dihedral angle deviations (see Materials and Methods). We have confirmed that changing the threshold values of this definition has a small effect on the computed relative binding free energy from Eq. (4). We have confirmed that the members of the defined binding-competent ensemble closely match the target crystal structure of the complex (1TJG) in terms of both structural and energetic features.

The computed relative binding free energies from Eq. (4) are compared to the experimental relative binding free energies from the fluorescence quenching measurements in Table 2. The modeling results, based on the computed reorganization free energies (Eq. (4)), reproduce the superior binding affinity of the B1 and C1 chimeric viruses for 2F5 relative to 14-C40-1. In general agreement with the measured values, the binding affinities of the C1 and B1 viruses are predicted to be approximately 2 kcal/mol more favorable than that of 14-C40-1, with the B1 virus slightly more favored than C1 (Table 2).

Model of B1:2F5 complex

We have constructed a structural model of the complex of the B1 virus with the 2F5 Fab using the computed conformation of B1 closest to the target crystal structure. We superimposed the ELDKWA residues of this conformation on the corresponding residues of the 1TJG crystal structure of the peptide:2F5 Fab complex (Fig. 4). In this model the ELDKWA epitope exhibits a remarkable shape complementarity with the 2F5 paratope, as evidenced by the amount of buried surface area of the ELDKWA motif in the complex. The ELKDWA motif is folded in a type I β-turn conformation that superimposes well on the crystal structure of the complex of the ELDKWA peptide with the 2F5. The interactions between the B1 chimeric virus and the antibody are mostly concentrated at the center of the epitope where the DKW core makes contacts with the corresponding paratope of 2F5 (Fig. 4). The interface between the two binding partners is predominantly hydrophobic with interaction between W666 of B1 and P98 of 2F5 and, to a lesser extent, with V100. A salt bridge between D664 of B1 and R95 of 2F5 is also present. The main chain of D664 interacts with the aromatic ring of Y94 of the light chain. Notably, the residues at the C-terminal end of ELDKWA assume an α-helical conformation, previously shown to be crucial for interaction with 2F5.[21,22] The model for the B1:2F5 complex shows how binding can occur without interference with the long CDR H3 finger of 2F5, which would otherwise prevent the formation of a high-affinity complex by clashing with the virus capsid. A similarly good fit was observed for the model of the cHRV3 chimeric virus in complex with the 2F5 Fab,[16] indicating that, in both cases, the flanking residues induce epitope conformations suitable for 2F5 recognition.

Discussion and Conclusions

We have analyzed the antigenic properties of isolates from a combinatorial library of HRV:HIV chimeric viruses displaying the ELDKWA epitope of the MPER of the gp41 transmembrane glycoprotein of HIV. The design of the library was based on the results of modeling calculations that identified a number of energetic and steric factors affecting the conformational propensities of the ELDKWA insert onto the HRV virus and its ability to assume conformations capable of fitting into the complementary determinant region of 2F5. From this library, we have been able to isolate a number of promising chimeras that bind 2F5 with greater affinity than that obtained earlier.

Remarkably, in a competitive ELISA, four of the five chimeras tested from this library bound 2F5 with greater affinity than one of the best binding chimeras from a previous library (14-C40-1, which also elicited diverse neutralizing anti-HIV antibodies when immunized with an ELDKWA-based peptide).[9] Fluorescence quenching measurements showed that the best among the chimeras analyzed, B1, binds to 2F5 400 times more strongly than does 14-C40-1. The difference in epitope sequence between the two constructs (ALDKWA in 14C40-1 and ELDKWA in B1 and C1) is likely unrelated to the variations in binding affinities observed in this work because the mutation of a pseudovirus from E to A did not interfere with neutralization.3 Molecular dynamics simulations of the B1, C1 and 14-C40-1 chimeras confirm the crucial role of the favorable conformational propensities of the inserts that are responsible, in part, for the corresponding gain in binding affinity.

Our results for the B1 chimera indicate a dissociation constant in the nanomolar range, similar to that measured for the free ELDKWA peptide.[17,23] This correspondence is consistent with the reorganization free energy we propose. The present computational result, together with our earlier analysis,[16] suggests that the free peptide and the B1 epitope have similar propensities for adopting binding-competent conformations. The key result of this work is to show that it is possible to display the epitope on HRV in conformations favoring high-affinity binding despite the structural restraints present at the insertion site. It is useful to compare the binding affinities to 2F5 measured for the HRV chimeras studied in this work with those corresponding to systems closer to the native environment. The affinity of B1 for 2F5 (K_d 2 nM) is similar to those (K_d 0.35–1.39 nM) between the 2F5 Fab and trimeric MPER constructs designed to mimic the intermediate conformation of gp41, which is believed to be the target of the 2F5 mAb *in vivo*.[24,25] This correspondence between the affinity of 2F5 for the engineered HRV chimeras and the trimeric MPER suggests, according to the conformational reorganization free energy model proposed, that the ELDKWA epitope is displayed on B1 in a conformation similar to that in the native environment.

The value of this work lies in the demonstration that, when properly employed, computational tools can be a useful complement to more experimental methods of protein design[26] by making it possible to test hypotheses *in silico* and pursue the hypotheses with subsequent focused experimental testing *in vitro*. The agreement between computed and observed binding affinities highlights the usefulness of the free energy reorganization model in rationalizing the epitope binding trends and confirms the validity of atomistic models as a tools to design *de novo* chimeric viruses that are likely to bind well *in vitro* and might lead to more timely identification of useful candidates for vaccine development.

The relative binding affinities from fluorescence quenching are greater than the corresponding computed values (relative free energy differences of −3.50 *versus* −2.01 kcal/mol for B1 and −2.02 *versus* −1.82 kcal/mol for C1 relative to 14-C40-1). This quantitative discrepancy can be attributed to a number of methodological factors, including limitations of the accuracy of the potential model used in the simulations. It could be interpreted also as an indication that conformational reorganization of the epitope, which is the only quantity probed by the calculations, is quantitatively important but not the only factor influencing the observed binding free energy differences. Other factors, such as binding-interaction energies and antibody reorganization, can contribute to variations in binding affinity. Our results indicate that in this case differences in conformational reorganization are more important for determining relative antibody affinities than other factors that are not modeled in the simulations.

The prediction accuracy of the atomistic molecular dynamics simulations we have used is limited by their ability to properly sample conformational space and by the reliability of the

energy function. Assumptions inherent in the model concerning the solution environment (pH, salt and cosolvent concentrations, etc.) can further limit the fidelity of computational models.

We recognize that strong binding affinity between HRV chimeric viruses and the 2F5 mAb (antigenicity) does not guarantee the ability of the chimeras to elicit the production of neutralizing antibodies against HIV (immunogenicity).[25] For instance, the viral membrane, which has not been considered in this work, has been hypothesized to play an important role in the binding of the epitope to 2F5.27 Separate immunization and HIV neutralization assays in animal models are needed to probe the immunogenicity of these chimeric viruses in eliciting neutralizing responses against HIV.

In conclusion, this study presents the application of a computational approach to quantitatively estimate binding affinities of chimeric viruses to the 2F5 mAb. The simulated binding affinities agree well with both forms of spectroscopic measurements used in this study. In addition, we have identified a chimeric HRV:HIV virus, B1, with a significantly enhanced binding affinity ($\Delta\Delta G$ – 3.5 kcal/mol) relative to one of the best binding chimeras (14-C40-1) previously characterized. The improved antigenic properties of B1 virus make this antigen a very attractive candidate for immunogenicity studies. The molecular design of B1 has proved that it is possible to improve the ability of antigens to bind specifically with complementary antibody based on structural insights, which is an important part of rational vaccine design.

Materials and Methods

Cells, viruses, plasmids, and media

H1-HeLa cells5 were used for the production, propagation, titering, and immunoselection of both wild-type HRV14 and recombinant HRV14:HIV-1 gp41 ELDKWAS chimeric viruses. 28 Media M and PA[11] were used with 1–10% (v/v) fetal bovine serum for plaque isolations and virus propagations. Dulbecco's modified Eagle medium (DMEM; Gibco, BRL, Carlsbad, CA) was used for HeLa cell transfection experiments. The bacterial strain used for transformation of the engineered plamids was *Escherichia coli* DH10B ElectroMax (Gibco, BRL, Carlsbad, CA). The pST-LIC plasmid, which was used for all genetic engineering, differs from the HRV-encoding p3IIST plasmid[29] used earlier in the engineered region (i.e. the region encoding the VP2 puff of the NIm-III region). In pST-LIC, the unique ApaI site was replaced with a BseRI site that could be digested first with BseRI and then with bacteriophage T4 DNA polymerase. This polymerase has 3′→5′ exonuclease activity in the absence of dNTPs, which allowed us to silently engineer the HRV sequences that flank the recombinant inserts to have an 11–15 sequence devoid of C or G residues (depending on the DNA strand) to allow the generation of 11–15 base sticky ends (in the presence of dCTP or dGTP). This plasmid promotes efficient mutagenesis with foreign inserts with complementary sticky ends.

Monoclonal antibodies and peptides

The broadly neutralizing human mAb 2F5 (PolyMun, Inc., Vienna), which binds the gp41 MPER epitope ELDKWA,30 was used for immunoselection and antigenicity assays. Murine mAb 17, which binds to the neutralizing immunogenic site IA (NIm IA) of HRV14,15 was used for ELISAs of chimeric HRV. Horseradish peroxidase-conjugated goat-anti-mouse IgG (Cappel ICN, Irvine, CA) was used for detection of chimeric HRVs. Ac-EQELLELDKWASSLW-NH_2 peptide, synthesized by NeoMPS, Inc. (San Diego, CA), was used for competition in ELISAs and for elution of the chimeric viruses in competitive immunoselections.

Design and generation of chimeric HRV14:ELDKWA library

The combinatorial library described was designed following the molecular simulation study that led to the inception of the cHRV3 construct.[16] A ligation-independent cloning method was used in which the pST-LIC plasmid was digested with BseRI and T4DNA polymerase to generate long sticky ends. A complementary recombinant insert was prepared for hybridization with the plasmid by first hybridizing two DNA oligonucleotides (synthesized by IDT, Piscataway, NJ) overlapping in the ELDKWAS-encoding region using codons preferred by the HRV14 RNA polymerase (Fig. 5). To optimize the binding of the foreign epitope to 2F5, the non-overlapping regions of the DNA oligomers encoded two randomized residues on each side of the ELDKWAS sequence (Table 1). Beyond these sequences were the sequences encoding the adjacent HRV14 residues to provide the sticky ends for hybridizing with the plasmid. The hybridized oligonucleotides were extended (using each of the dNTPs and Klenow DNA polymerase I (New England Biolabs, Beverly, MA)), treated with T4 DNA polymerase (and dCTP or dGTP to generate the complementary sticky ends), and allowed to hybridize in a 10:1 ratio with the prepared vector. Electroporation of DH10B *E. coli* cells was performed using a Gene Pulser system (Bio-Rad laboratories, Hercules, CA) according to the manufacturer's instructions (25 μF, 200 V, 200 A). Transformed cells were grown in bulk liquid cultures at 30 °C to late log phase and then harvested using Qiagen Mini-Prep Spin Kits (Valencia, CA). After linearizing the pools of recombinant plasmids with MluI, plasmids were transcribed *in vitro* using AMBION MegaScript kits (Austin, TX). Full-length RNA transcripts were transfected into H1-HeLa cells by electroporation (10 μL of the infectious RNAs added to 1×10^7 of H1-HeLa cells in 400 μL of D-MEM and then placed in a 0.4 cm Gibco-BRL electroporation cuvette and electroporated at 250 V, 960 μF. The resultant chimeric viruses were harvested as described.[11]

Partial purification of virus libraries and viral isolates

A protocol developed by Zhang *et al.*[31] was followed for the partial purification of the combinatorial virus library as well as individual viruses. After three cycles of freezing and thawing, infected cells were harvested, concentrated and the suspension was centrifuged (to remove cell wall debris), after which the clarified lysates were subjected to treatment with DNase I followed by ultracentrifugation (with a 30% (w/v) sucrose cushion) at 42,000 rpm for 2.5 h at 15 °C in a Beckman 45 Ti rotor. Pellets were suspended in 20 mM Tris–HCl, pH 7.4 and contained the chimeric viruses as well as some cell-derived ribosomes.

Immunoselection of viruses

Immunosorp plates (96 well; Nunc, Rochester, NY) were coated with mAb 2F5 to immunoselect chimeric rhinovirus pools from the new library, essentially as described.[12] After incubation at 4 °C overnight, the plates were washed and blocked with 3% (w/v) gelatin in phosphate-buffered saline (PBS). After incubation for 1 h at 37 °C, the plates were washed six times with PBS-T (PBS containing 0.05% (v/v) Tween 20). Serial dilutions of the competing peptide Ac-EQELLELDKWASSLW-NH_2, yielding 0, 2, 4, 8, 16 pmol/well, were prepared and 3×10^5 plaque-forming units of the chimeric virus library were added. The plates were incubated for 2 h at 37 °C, washed six times with PBS-T and then 2×10^4 H1-HeLa cells in medium M with 10% (v/v) FBS were added to each well. The plates were incubated for 70 h at 34.5 °C in an atmosphere of 2.5% (v/v) CO_2 and cells were harvested when they displayed 80% cytopathic effect (CPE). The harvested cells were lysed by three cycles of freezing and thawing and then centrifuged to produce clarified virus lysates.

Plaque isolation and sequencing

Individual viral isolates were obtained as described.[17] Plaque purification was done twice to minimize contamination by additional viruses. QIAamp viral RNA purification kits were used

to extract the viral RNA of chimeric viruses according to the manufacturer's instructions. The resulting DNA was analyzed by electrophoresis in a 2% (w/v) agarose gel. QIAquick gel extraction kits (Valencia, CA) were used to purify the products, which were sequenced at the UMDNJ-RWJMS DNA Core Facility (Piscataway, NJ).

Competitive enzyme-linked immunosorbent assays (ELISAs) of chimeric viruses

Competitive ELISAs were done in triplicate using immobilized mAb 2F5 essentially as described[9] with the exception that 3×10^5 plaque-forming units of virus were mixed with the 14-mer ELDKWA-containing peptide in serial dilutions before being added to the immobilized 2F5 for 120 min at 37 °C. The anti-HRV14 mAb 17 was then added, incubated, and washed before treatment with horseradish peroxidase-conjugated goat anti-mouse IgG (at a 1:10,000 dilution). This was incubated, washed, and treated with, peroxidase substrate (0.3 mg/mL tetramethylbenzidine dissolved in 10% dimethyl sulfoxide, 0.18 M sodium citrate, pH 3.95). The color reaction was obtained by adding H_2O_2 to 0.001% (v/v), and then stopped by adding an equal volume of 4 M H_2SO_4, and the absorbance at 450 nm (A_{450}) was measured. It was expected that the presence of the competing peptide would lead to more stringent conditions, promoting the binding of 2F5 to only those chimeras displaying ELDKWA in conformations better resembling those of the native epitope than the peptide. The binding free energies of the B1 and C1chimeras relative to 14-C40-1 were estimated from the ELISA data as:

$$\Delta\Delta G_i = -kT\ln C_i/C_{14-C40-1}$$

where C_i is the concentration of the peptide at A_{450} =0.5 for the corresponding chimera. The statistical uncertainties of the ELISA-derived ΔΔG's were obtained by error propagation.

Fluorescence measurements

Fluorescence quenching experiments were used to measure the binding constants between the mAb 2F5 and selected chimeric viruses. The fluorescence spectra were obtained using a spectrofluorimeter equipped with a quartz cuvette of 1 cm path length and a thermally controlled cell holder.[32] The fluorescence emission (λem) spectra were recorded from 300 nm to 450 nm, with the path length for fluorescence excitation and emission of 5 mm, at an excitation wavelength (λex) of 280 nm. Virus–antibody binding was monitored by changes in the fluorescence emission intensity recorded at 370 nm. Changes in intrinsic fluorescence of viruses and antibody fragments were used to monitor ligand binding at 25 °C by titration with mAb 2F5. All virus and antibody solutions were prepared in 20 mM Tris–HCl, pH 7.2 made with deionized H_2O. All titrations were done with the same amounts of 2F5 added to a fixed concentration of protein, holding the concentration of chimeric viruses B1, C1, and 14-C40-1 at 1 nM. To cover the broad range of ligand concentration, stock solutions with concentrations of 2F5 ranging from 6.74×10^{-9} to 1.04×10^{-6} M were used. Freshly prepared 2 mL solutions of B1, C1, and 14-C40-1 (in 20 mM Tris–HCl, pH 7.2) at the desired concentration were placed into the cuvette, 1 μL of 2F5 solution was added and the mixture was stirred. Values are reported as the average of two independent measurements for the experiments done in the presence of chimeric virus (Fig. 5b). We calculated the dissociation constant (K_d) by fitting the 2F5-induced changes in fluorescence using the following formula:[32]

$$I = I_0 + {}^0\frac{(I_\infty - I_o)}{2[D]_{tot}}\left[([D]_{tot}+[R]_{tot}+K_d) - \sqrt{([D]_{tot}+[R]_{tot}+K_d)^2 - 4[D]_{tot}[R]_{tot}}\right]$$

In this relationship, I_0 and I are the fluorescence emission intensity of the virus in the absence and in the presence of antibody, respectively; I_∞ is the fluorescence emission intensity of the

virus at saturation; and $[D]_{tot}$ and $[R]_{tot}$ are the total concentrations of epitope and antibody, respectively. The statistical standard error estimates for K_d were obtained by non-linear regression analysis based on the error bounds of the fluorescence intensities.

Replica exchange molecular dynamics

The temperature replica exchange molecular dynamics (REMD) method[33–35] as implemented in the IMPACT computational package[36] was used in this work to explore the predicted conformational space of several peptide sequences derived from the MPER of HIV gp41 and inserted into the HRV14 viral capsid. REMD is an advanced canonical conformational sampling algorithm designed to help overcome the sampling problem encountered in biomolecular simulations. It consists of running a series of MD simulations of the molecular system in parallel over multiple processors at different temperatures. Periodically, a Monte Carlo move is attempted, aimed at swapping atomic coordinates of one replica with those of another. Typically, the lowest temperature replica corresponds to the temperature of interest and the high temperature replicas allow a rapid exploration of the extent of conformational space. In the temperature replica exchange method, efficient interconversion among low-energy conformations occurs whereby the temperature switches from low to high, allowing the conformation to overcome potential energy barriers and then transition to another conformation. A new low-energy conformation can then be established when this conformation transfers back to low temperature replicas.

Force-field and implicit solvation model

All simulations employed the OPLS-AA fixed charge all-atom force field[37,38] and the AGBNP[19] implicit solvent model to mimic the water environment. Simulations using implicit solvent models are not as computationally intensive as those using explicit solvent models. This is particularly true for REMD simulations because far fewer replicas are needed to achieve reasonable replica exchange rates due to the smaller system and broader overlap of the energy distributions among replicas at different temperatures. AGBNP is an implicit solvent model based on a novel implementation of the pairwise descreening scheme of the generalized Born model[39,40] for the electrostatic component, and a novel non-polar hydration-free energy estimator. The non-polar term consists of an estimator for the solute solvent van der Waals dispersion energy designed to mimic explicit solvent solute-solvent van der Waals interaction energies in addition to a surface area term corresponding to the work required for cavity formation. It has been used to study protein conformational equilibrium and protein allostery.[41]

Model preparation

The B1 and C1 HRV14:HIV chimeric constructs investigated in this work were obtained by insertion of gp41-derived epitopes into the βE-βF region of the so-called VP2 puff of the VP2 subunit of the HRV14 protomeric unit, the largest of three loops forming the neutralizing immunogenic site II (NIm-II) of HRV14 (Table 1).[13,14] The chimeric cHRV3 construct[16] contains the sequence ELDKWAS inserted between the N160 and E161 residues of VP2, without the removal of any HRV14 residue or the addition of any flanking residue. The new chimeric virus library from which the B1 and C1 chimeras were isolated differs from the cHRV3 chimera in that the two HRV residues flanking the ELDKWAS insert were randomized instead of being limited to the HRV14 AN and EV residues (Table 1). Starting structures were obtained by homology modeling using the program Prime[42] (Schrodinger, Inc.) and the structure of wild-type HRV14 (PDB ID 4RHV) as a structural template (97% sequence identity). The energy-minimized models were assessed for quality using ProCheck, indicating 84.6%, 14.6%, 0.7%, and 0.1% in the most favored regions, allowed regions, generously allowed regions, and disallowed regions of the Ramachandran plot, respectively.[43]

REMD simulations of the chimeric constructs

REMD simulations of the B1 and C1 viral constructs were done to estimate the conformational propensities of the inserts. The production REMD runs, consisting of 30 replicas with temperatures in the range 310–495 K, were 5 ns per replica in length for a total of 60 ns for each system. The production runs were preceded by minimization and equilibration calculations starting with the comparative models described above. To reduce computational complexity, the model included only the HRV14 residues (including those from the VP1 and VP3 subunits) that contained atoms within 20 Å from any atom of the foreign insert and, furthermore, only the 176 residues closest to the insert were allowed to move. The positions of C^{α} atoms of the residues at the ends of dangling protein chains were harmonically restrained using an isotropic force constant of 0.3 kcal $mol^{-1}Å^{-2}$. This setup prevents unfolding of the simulated protein region at high temperature while providing a reasonable description of the protein environment surrounding the inserted sequence. This methodology was tested by applying it to the chimeric HRV displaying part of the HIV-1 V3 loop of the MN-III-2 chimera studied by Smith *et al.*[12] and by Ding *et al.*[44] We confirmed that the main cluster of conformations of the loop generated by REMD structurally matched that of the crystal structure.

Algorithm to detect conformer similarity

We have used a structural criterion to select conformers of the simulated ensembles of B1, C1, and 14-C40-1 that match closely to the ELDKWA peptide conformation bound to the 2F5 Fab (1TJG). A conformation belongs to this binding-competent macrostate if it is within 2 Å C^{α} RMSD and within 30° of the backbone angles of DKW relative to the peptide in 1TJG. This analysis allowed us to define the population of the bound state and to estimate the free energy of reorganization ($\Delta\Delta G_{calc}$) from the REMD simulation. Statistical uncertainty for the populations was obtained by means of a Bayesian inference analysis based on the counts of binding-competent conformations and the total numbers of samples as described.[45]

Supplementary Material

Refer to Web version on PubMed Central for supplementary material.

Abbreviations used

cHRV	chimeric rhinovirus
Fab	antigen-binding fragment
HIV	human immunodeficiency virus
HRV	human rhinovirus
mAb	monoclonal antibody
MPER	membrane-proximal external region
NIm-II	neutralizing immunogenic site II
REMD	temperature replica exchange molecular dynamics

Acknowledgments

This work was supported, in part, by NIH grant GM30580 (to R.M.L.) and by NIH grant AI071874 (to G.F.A.). The computer simulations for this work were done at the BioMaPS High Performance Computing Center at Rutgers University and funded, in part, by National Institute of Health shared instrumentation grant no. 1 S10 RR022375. We are grateful to Thomas Mariano and Rachel Bradley for their assistance with cell cultures, and to Chris Barbieri for assistance with the fluorescence experiment.

References

1. Karlsson Hedestam GB, Fouchier RA, Phogat S, Burton DR, Sodroski J, Wyatt RT. The challenges of eliciting neutralizing antibodies to HIV-1 and to influenza virus. Nat. Rev. Microbiol 2008;6:143–155. [PubMed: 18197170]
2. Alfsen A, Bomsel M. HIV-1 gp41 envelope residues 650–685 exposed on native virus act as a lectin to bind epithelial cell galactosyl ceramide. J. Biol. Chem 2002;277:25649–25659. [PubMed: 11940580]
3. Zwick MB, Jensen R, Church S, Wang M, Stiegler G, Kunert R, et al. Anti-human immunodeficiency virus type 1 (HIV-1) antibodies 2F5 and 4E10 require surprisingly few crucial residues in the membrane-proximal external region of glycoprotein gp41 to neutralize HIV-1. J. Virol 2005;79:1252–1261. [PubMed: 15613352]
4. Penn-Nicholson A, Han DP, Kim SJ, Park H, Ansari R, Montefiori DC, Cho MW. Assessment of antibody responses against gp41 in HIV-1-infected patients using soluble gp41 fusion proteins and peptides derived from M group consensus envelope. Virology 2008;372:442–456. [PubMed: 18068750]
5. Muster T, Guinea R, Trkola A, Purtscher M, Klima A, Steindl F, et al. Cross-neutralizing activity against divergent human immunodeficiency virus type 1 isolates induced by the gp41 sequence ELDKWAS. J. Virol 1994;68:4031–4034. [PubMed: 7514684]
6. Cardoso RM, Zwick MB, Stanfield RL, Kunert R, Binley JM, Katinger H, et al. Broadly neutralizing anti-HIV antibody 4E10 recognizes a helical conformation of a highly conserved fusion-associated motif in gp41. Immunity 2005;22:163–173. [PubMed: 15723805]
7. Pejchal R, Gach JS, Brunel FM, Cardoso RM, Stanfield RL, Dawson PE, et al. A conformational switch in human immunodeficiency virus gp41 revealed by the structures of overlapping epitopes recognized by neutralizing antibodies. J. Virol 2009;83:8451–8462. [PubMed: 19515770]
8. Matyas GR, Wieczorek L, Beck Z, Ochsenbauer-Jambor C, Kappes JC, Michael NL, et al. Neutralizing antibodies induced by liposomal HIV-1 glycoprotein 41 peptide simultaneously bind to both the 2F5 or 4E10 epitope and lipid epitopes. AIDS 2009;23:2069–2077. [PubMed: 19710597]
9. Resnick DA, Smith AD, Gesiler SC, Zhang A, Arnold E, Arnold GF. Chimeras from a human rhinovirus 14-human immunodeficiency virus type 1 (HIV-1) V3 loop seroprevalence library induce neutralizing responses against HIV-1. J. Virol 1995;69:2406–2411. [PubMed: 7884887]
10. Smith AD, Geisler SC, Chen AA, Resnick DA, Roy BM, Lewi PJ, et al. Human rhinovirus type 14:human immunodeficiency virus type 1 (HIV-1) V3 loop chimeras from a combinatorial library induce potent neutralizing antibody responses against HIV-1. J. Virol 1998;72:651–659. [PubMed: 9420270]
11. Arnold E, Rossmann MG. Analysis of the structure of a common cold virus, human rhinovirus 14, refined at a resolution of 3.0 Å. J. Mol. Biol 1990;211:763–801. [PubMed: 2156077]
12. Arnold GF, Velasco PK, Holmes AK, Wrin T, Geisler SC, Phung P, et al. Broad neutralization of human immunodeficiency virus type 1 (HIV-1) elicited from human rhinoviruses that display the HIV-1 gp41 ELDKWA epitope. J. Virol 2009;83:5087–5100. [PubMed: 19279101]
13. Gallichan WS, Johnson DC, Graham FL, Rosenthal KL. Mucosal immunization with a recombinant adenovirus vector induces local and systemic immunity and protection from herpes simplex virus. Adv. Exp. Med. Biol 1995;371:1581–1585. [PubMed: 7502860]
14. Rossmann MG, Arnold E, Erickson JW, Frankenberger EA, Griffith JP, Hecht HJ, et al. Structure of a human common cold virus and functional relationship to other picornaviruses. Nature 1985;317:145–153. [PubMed: 2993920]
15. Sherry B, Rueckert R. Evidence for at least two dominant neutralization antigens on human rhinovirus 14. J. Virol 1985;53:137–143. [PubMed: 2981332]
16. Lapelosa M, Gallicchio E, Arnold GF, Arnold E, Levy RM. In silico vaccine design based on molecular simulations of rhinovirus chimeras presenting HIV-1 gp41 epitopes. J. Mol. Biol 2009;385:675–691. [PubMed: 19026659]
17. Alam SM, McAdams M, Boren D, Rak M, Scearce RM, Gao F, et al. The role of antibody polyspecificity and lipid reactivity in binding of broadly neutralizing anti-HIV-1 envelope human

monoclonal antibodies 2F5 and 4E10 to glycoprotein 41 membrane proximal envelope epitopes. J. Immunol 2007;178:4424–4435. [PubMed: 17372000]

18. Dekker EL, Porta C, Van Regenmortel MH. Limitations of different ELISA procedures for localizing epitopes in viral coat protein subunits. Arch. Virol 1989;105:269–286. [PubMed: 2473721]
19. Ofek G, Tang M, Sambor A, Katinger H, Mascola JR, Wyatt R, Kwong PD. Structure and mechanistic analysis of the anti-human immunodeficiency virus type 1 antibody 2F5 in complex with its gp41 epitope. J. Virol 2004;78:10724–10737. [PubMed: 15367639]
20. Gallicchio E, Levy RM. AGBNP: an analytic implicit solvent model suitable for molecular dynamics simulations and high-resolution modeling. J. Comput. Chem 2004;25:479–499. [PubMed: 14735568]
21. Biron Z, Khare S, Samson AO, Hayek Y, Naider F, Anglister J. A monomeric 3(10)-helix is formed in water by a 13-residue peptide representing the neutralizing determinant of HIV-1 on gp41. Biochemistry 2002;41:12687–12696. [PubMed: 12379111]
22. Bryson S, Julien JP, Isenman DE, Kunert R, Katinger H, Pai EF. Crystal structure of the complex between the F(ab)′ fragment of the cross-neutralizing anti-HIV-1 antibody 2F5 and the F(ab) fragment of its anti-idiotypic antibody 3H6. J. Mol. Biol 2008;382:910–919. [PubMed: 18692506]
23. Tian Y, Ramesh CV, Ma X, Naqvi S, Patel T, Cenizal T, et al. Structure-affinity relationships in the gp41 ELDKWA epitope for the HIV-1 neutralizing monoclonal antibody 2F5: effects of side-chain and backbone modifications and conformational constraints. J. Pept. Res 2002;59:264–276. [PubMed: 12010517]
24. Frey G, Peng H, Rits-Volloch S, Morelli M, Cheng Y, Chen B. A fusion-intermediate state of HIV-1 gp41 targeted by broadly neutralizing antibodies. Proc. Natl Acad. Sci. USA 2008;105:3739–3744. [PubMed: 18322015]
25. Hinz A, Schoehn G, Quendler H, Hulsik DL, Stiegler G, Katinger H, et al. Characterization of a trimeric MPER containing HIV-1 gp41 antigen. Virology 2009;390:221–227. [PubMed: 19539967]
26. Sood VD, Baker D. Recapitulation and design of protein binding peptide structures and sequences. J. Mol. Biol 2006;357:917–927. [PubMed: 16473368]
27. Brunel FM, Zwick MB, Cardoso RM, Nelson JD, Wilson IA, Burton DR, Dawson PE. Structure-function analysis of the epitope for 4E10,a broadly neutralizing human immunodeficiency virus type 1 antibody. J. Virol 2006;80:1680–1687. [PubMed: 16439525]
28. Conant RM, Hamparian VV. Rhinoviruses: basis for a numbering system. II. Serologic characterization of prototype strains. J. Immunol 1968;100:114–119. [PubMed: 4295060]
29. Smith AD, Resnick DA, Zhang A, Geisler SC, Arnold E, Arnold GF. Use of random systematic mutagenesis to generate viable human rhinovirus 14 chimeras displaying human immunodeficiency virus type 1 V3 loop sequences. J. Virol 1994;68:575–579. [PubMed: 8254775]
30. Muster T, Steindl F, Purtscher M, Trkola A, Klima A, Himmler G, et al. A conserved neutralizing epitope on gp41 of human immunodeficiency virus type 1. J. Virol 1993;67:6642–6647. [PubMed: 7692082]
31. Zhang A, Nanni RG, Li T, Arnold GF, Oren DA, Jacobo-Molina A, et al. Structure determination of antiviral compound SCH 38057 complexed with human rhinovirus 14. J. Mol. Biol 1993;230:857–867. [PubMed: 8386772]
32. Barbieri CM, Kaul M, Pilch DS. Use of 2-aminopurine as a fluorescent tool for characterizing antibiotic recognition of the bacterial rRNA A-site. Tetrahedron 2007;63:3567–6574. [PubMed: 18431442]
33. Sugita Y, Okamoto Y. Replica-exchange molecular dynamics method for protein folding. Chem. Phys. Lett 1999;314:141–151.
34. Felts AK, Harano Y, Gallicchio E, Levy RM. Free energy surfaces of beta-hairpin and alphahelical peptides generated by replica exchange molecular dynamics with the AGBNP implicit solvent model. Proteins: Struct. Funct. Genet 2004;56:310–321. [PubMed: 15211514]
35. Gallicchio E, Levy RM, Parashar M. Asynchronous replica exchange for molecular simulations. J. Comput. Chem 2007;29:788–794. [PubMed: 17876761]
36. Banks JL, Beard HS, Cao Y, Cho AE, Damm W, Farid R, et al. Integrated modeling program, applied chemical theory (IMPACT). J. Comput. Chem 2005;26:1752–1780. [PubMed: 16211539]

37. Kaminski GA, Friesner RA, Tirado-Rives J, Jorgensen WL. Evaluation and reparame-trization of the OPLS-AA force field for proteins via comparison with accurate quantum chemical calculations on peptides. J. Phys. Chem. B 2001;105:6474–6487.

38. Jorgensen WL, Maxwell DS, Tirado-Rives J. Development and testing of the OPLS all-atom force field on conformational energetics and properties of organic liquids. J. Am. Chem. Soc 1996;118:11225–11236.

39. Qiu D, Shenkin PS, Hollinger FP, Still WC. The GB/SA Continuum model for solvation. A fast analytical method for the calculation of approximate born radii. J. Phys. Chem. A 1997;101:3005–3014.

40. Bashford D, Case DA. Generalized born models of macromolecular solvation effects. Annu. Rev. Phys. Chem 2000;51:129–152. [PubMed: 11031278]

41. Ravindranathan KP, Gallicchio E, Levy RM. Conformational equilibria and free energy profiles for the allosteric transition of the ribose-binding protein. J. Mol. Biol 2005;353:196–210. [PubMed: 16157349]

42. Guallar V, Jacobson M, McDermott A, Friesner RA. Computational modeling of the catalytic reaction in triosephosphate isomerase. J. Mol. Biol 2004;337:227–239. [PubMed: 15001364]

43. Laskowski RA, MacArthur MW, Moss DS, Thornton JM. PROCHECK: a program to check the stereochemical quality of protein structures. J. Appl. Crystallogr 1993;26:283–291.

44. Ding J, Smith AD, Geisler SC, Ma X, Arnold GF, Arnold E. Crystal structure of a human rhinovirus that displays part of the HIV-1 V3 loop and induces neutralizing antibodies against HIV-1. Structure 2002;10:999–1011. [PubMed: 12121655]

45. Gallicchio E, Andrec M, Felts AK, Levy RM. Temperature weighted histogram analysis method, replica exchange, and transition paths. J. Phys. Chem. B 2005;109:6722–6731. [PubMed: 16851756]

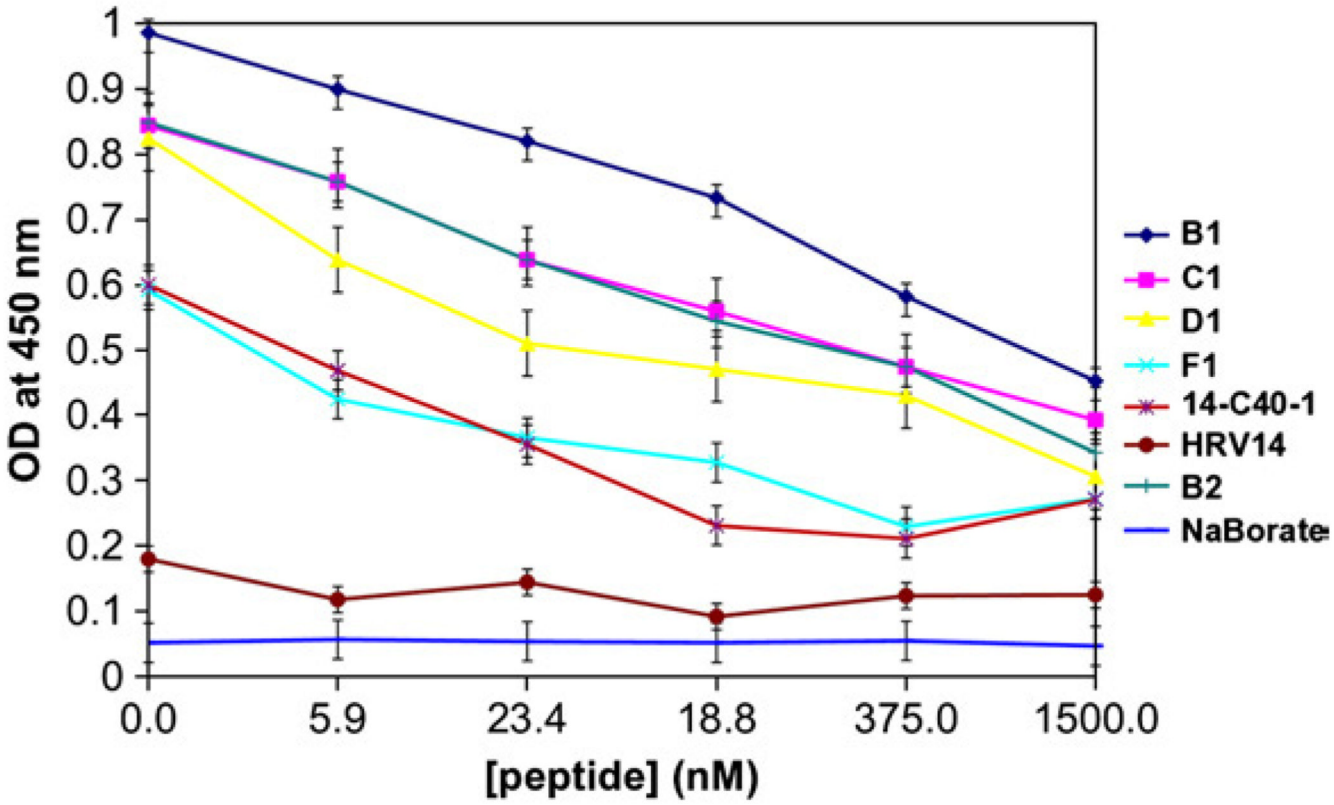

Fig. 1.

Competitive ELISA titers illustrating the competition of a 14-mer ELDKWA-containing peptide and a number of chimeric viruses for binding immobilized mAb 2F5. OD is the optical density (absorbance) and [peptide] is the concentration of the competitor peptide. Error bars represent the standard errors of the mean.

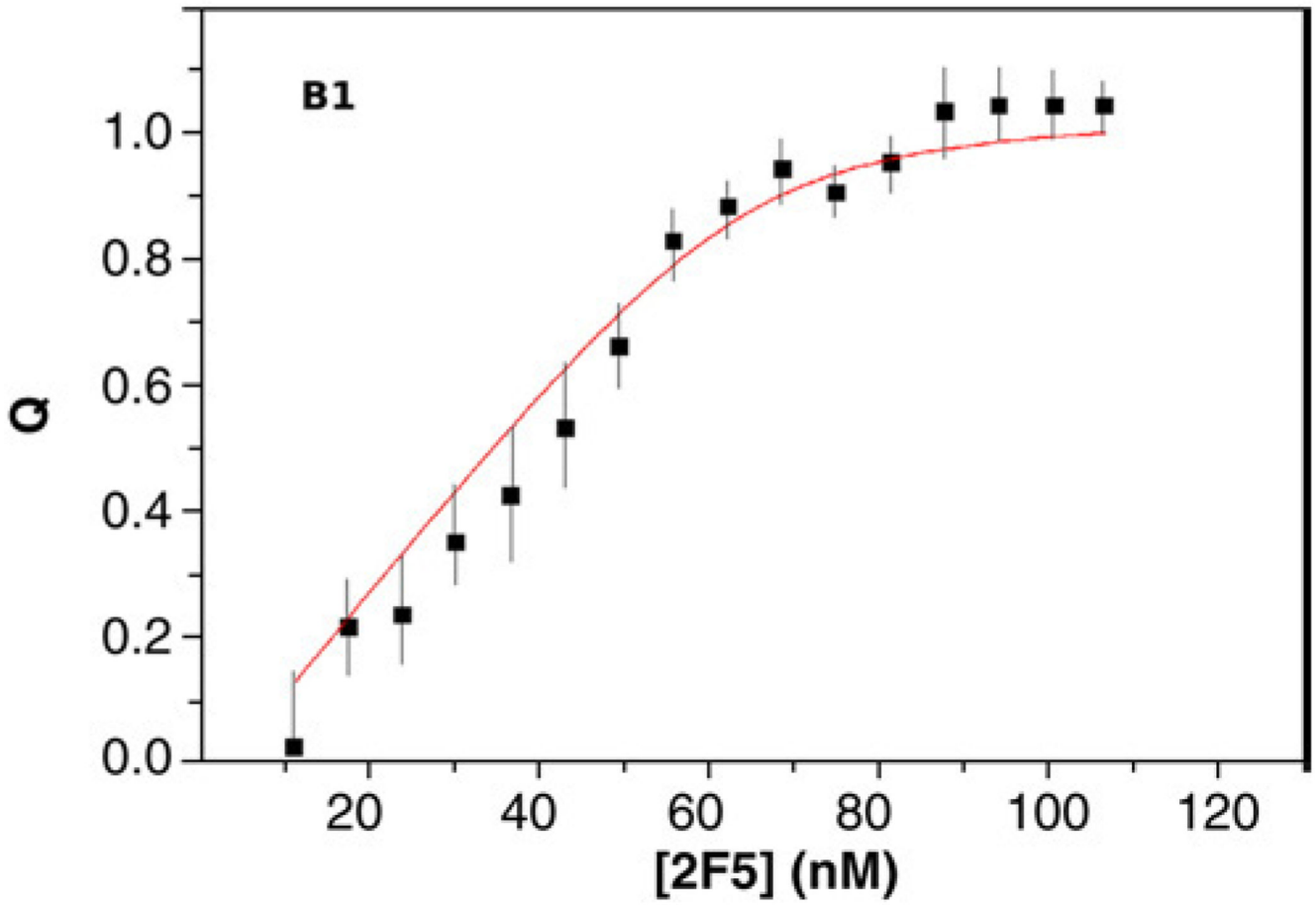

Fig. 2.

Fluorescence intensity curve for the B1 construct, determined as a function of the 2F5 mAb concentration, used to calculate the equilibrium dissociation constants, K_d (as described in Materials and Methods). The non-linear fitting curve is shown in red: $Q=(I-I_0)/(I_\infty-I_0)$. The corresponding curves for the C1 and 14-C40-1 constructs are similar in shape but shifted to higher concentrations of antibody, reflecting their lower affinities compared to B1. The goodness of fit is measured as χ^2 per degree of freedom (B1, 1.01; C1, 0.98; 14-C40-1, 0.8).

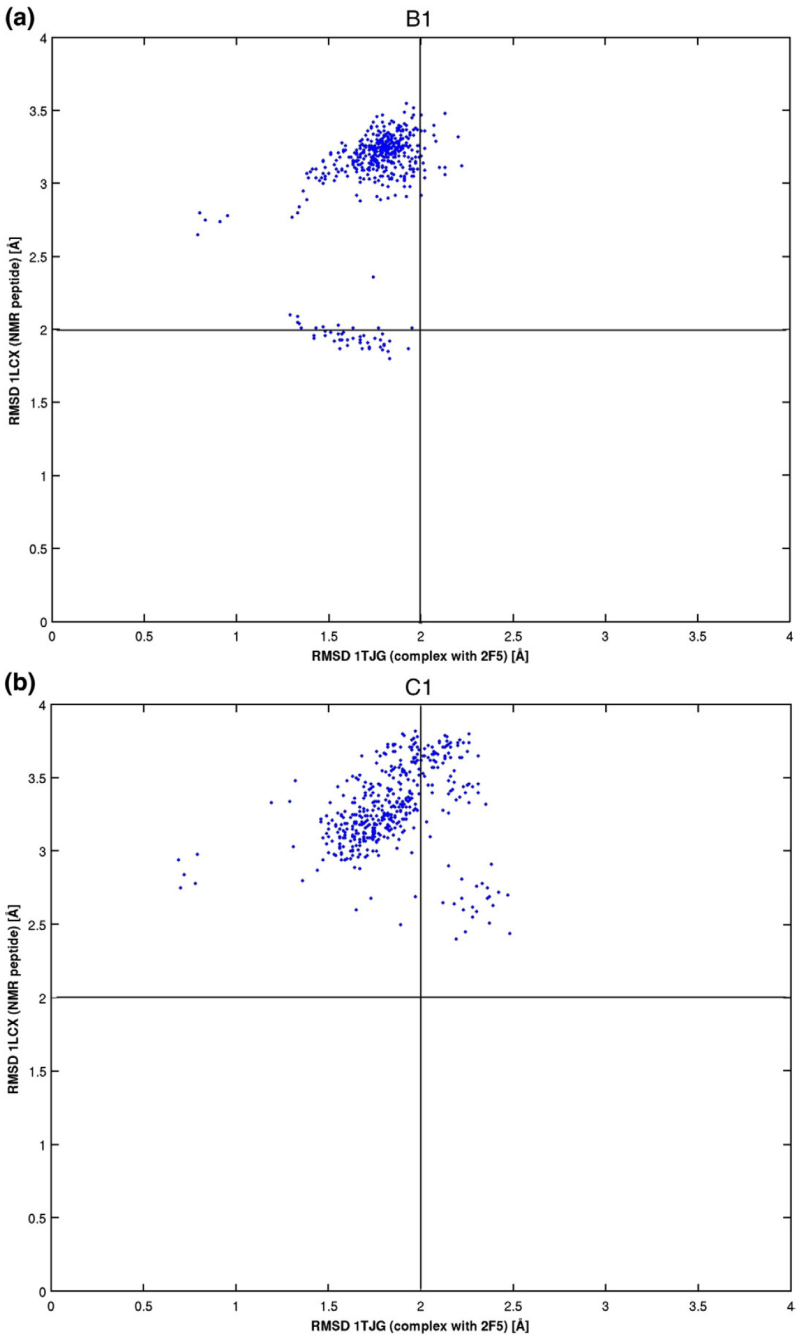

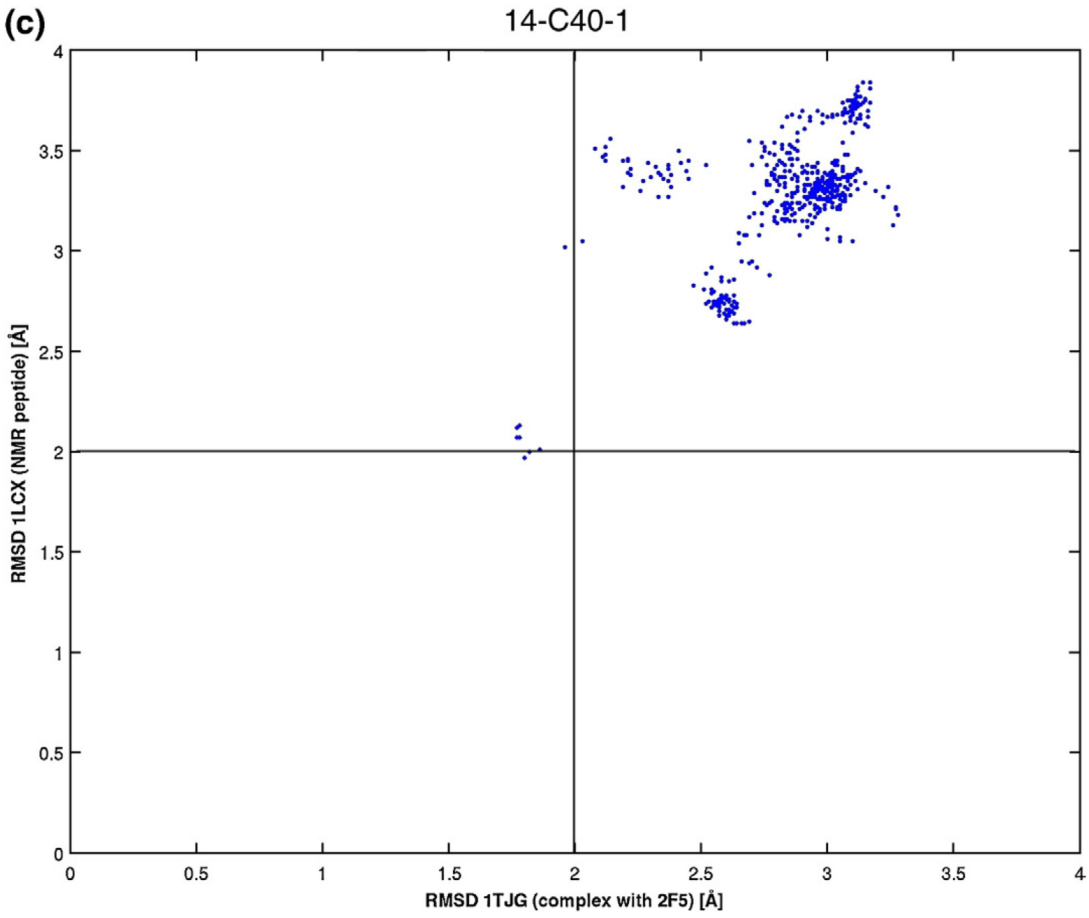

Fig. 3.

Scatter plot of the C^{α} RMSD values from the ELDKWA motif from the REMD ensembles of the chimeric viruses in solution at 310 K with respect to the same motif of the peptide in the 1TJG crystal structure (*x*-axis) and in the 1LCX NMR structure (*y*-axis). The B1 and C1 structures display primarily β-turn conformations, and the 14-C40-1 structures display turn conformations that are less similar to a canonical β-turn conformation.

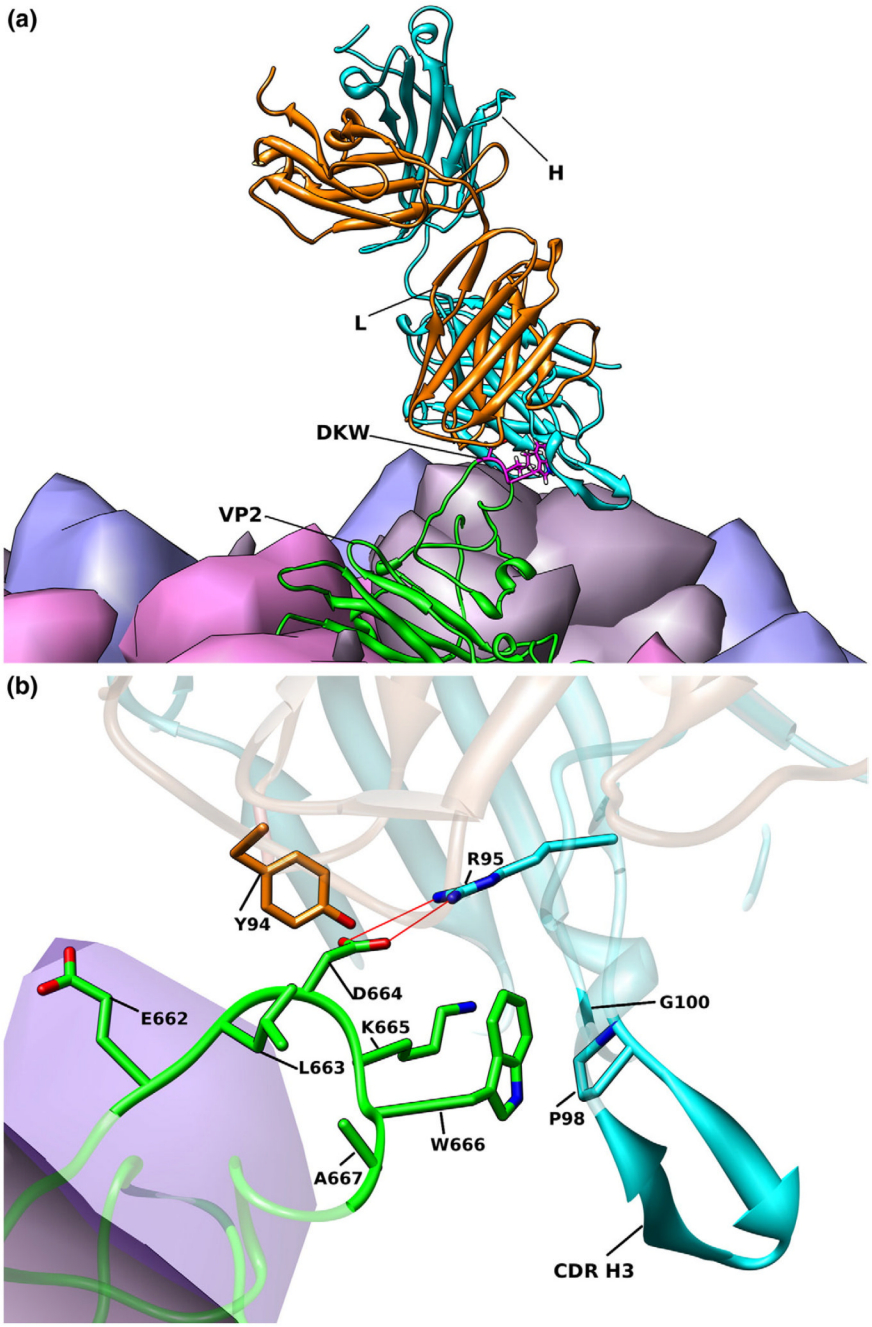

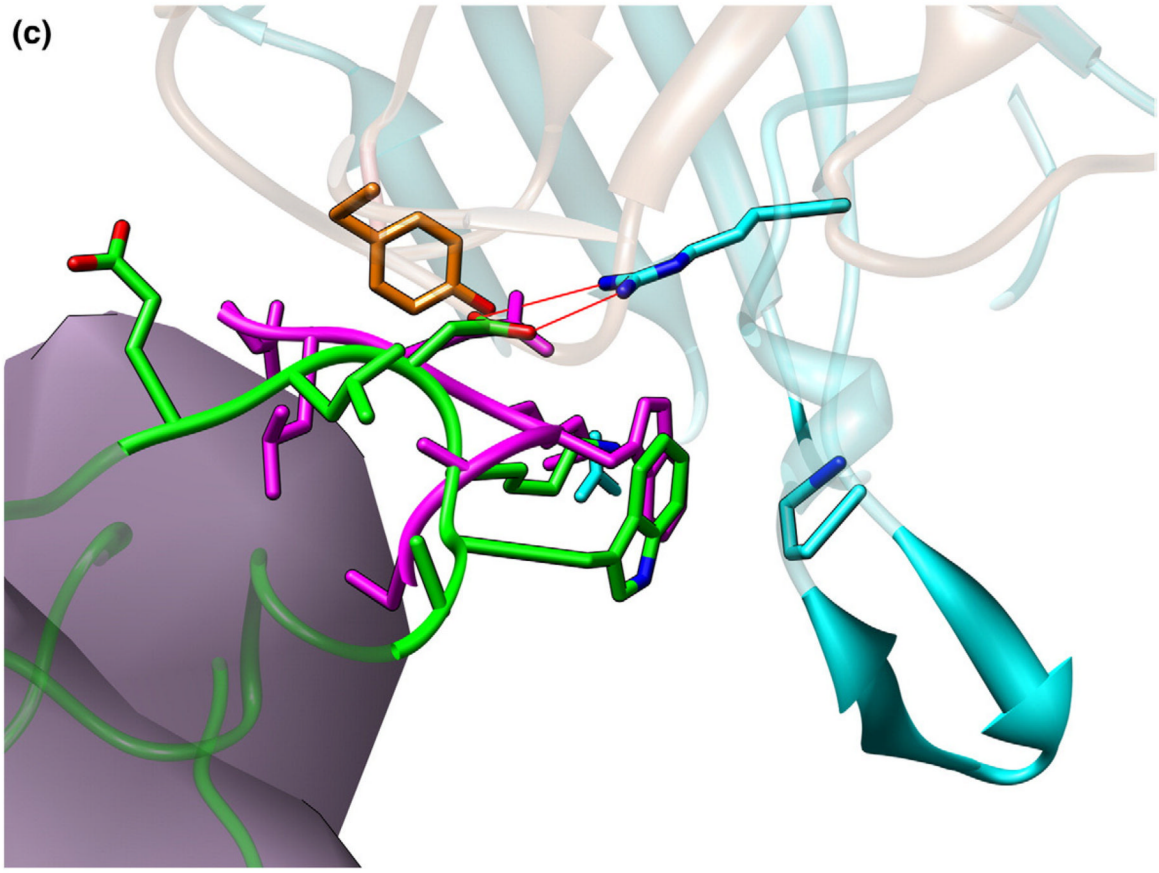

Fig. 4.

A model of the B1 chimera bound to the 2F5 Fab. (a) One of the VP2 subunits of the protomeric unit is shown in green. The Fab has a ribbon representation, with the light chain shown in orange and the heavy chain shown in cyan. The DKW motif of the 2F5 epitope is shown in a stick representation. (b) Close-up view of the binding region of the modeled B1:2F5 Fab complex. Residues of the ELDKWA motif and residues of the 2F5 within 7 Å are shown in stick representations, and the rest are depicted as ribbons, with VP2 in green and the heavy chain, including the H3 region, and the light chain of 2F5 shown in cyan and orange, respectively. The HIV-1 residues are numbered according to their HIV-1 HxB2 amino acid numbers. (c) As (b) with the modeled conformation of the ELDKWA peptide (magenta) in the crystal structure (1TJG) superimposed.

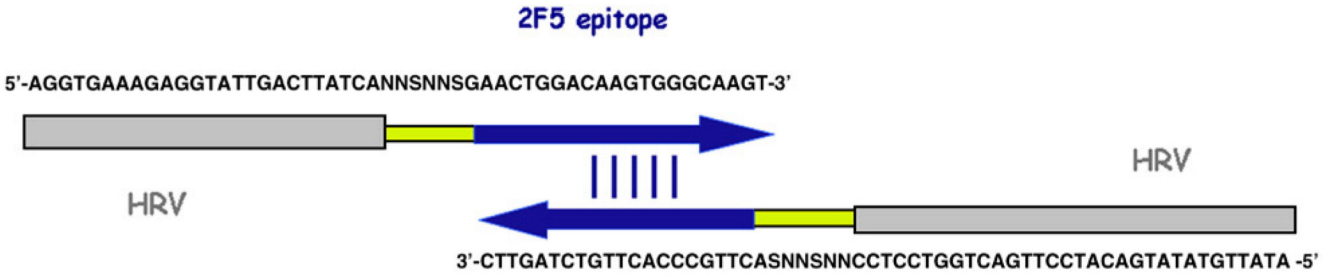

Fig. 5.

The DNA oligonucleotides for the forward and reverse primers used to generate the new combinatorial library. N, equimolar fractions of A, G, C, and T; and S, equimolar fractions of C and G.

Table 1

Chimeric libraries investigated in this work

Virus	HRV	N-linker	2F5 epitope	C-Linker	HRV
14-C40-1[a]	DLS	PCG	ALDKWAS	SPDCS	VGGP
cHRV3[b]	DLSSAN	—	ELDKWAS	—	EVGGP
Library[c]	DLSS	XX[d]	ELDKWAS	XX	GGP
Individual immunoselected viruses from library					
B1	DLSS	HG	ELDKWAS	PN	GGP
C1	DLSS	PG	ELDKWAS	IP	GGP
D1	DLSS	SP	ELDKWAS	LP	GGP
F1	DLSS	PP	ELDKWAS	SP	GGP
B2	DLSS	GK	ELDKWAS	QP	GGP

[a] One of the previous best binders to 2F5.

[b] The modeled chimera predicted to bind 2F5 with greater affinity than 14-C40-1.

[c] The library composition (this work).

[d] X, any of the 20 amino acids.

Table 2

Relative binding free energies of the B1 and C1 chimeric viruses to the 2F5 mAb with respect to 14-C40-1 as measured by competitive ELISA (Fig. 1) and fluorescence quenching (Fig. 2), and as calculated

	ΔG_{obs} fluorescence (kcal/mol)	$\Delta\Delta G_{obs}$ fluorescence (kcal/mol)	$\Delta\Delta G_{obs}$ ELISA (kcal/mol)	$\Delta\Delta G_{calc}$ (kcal/mol)
B1	−11.82±0.1	−3.51±1.0	−2.95±0.21	−2.01±0.51
C1	−10.36±0.1	−2.05±1.0	−1.90±0.25	−1.82±0.52
14-C40-1	−8.31±0.9	0[a]	0[a]	0[a]

[a]Reference chimera.